HHS Public Access

Author manuscript

J Biomech. Author manuscript; available in PMC 2023 April 01.

Published in final edited form as:

J Biomech. 2022 April ; 135: 111023. doi:10.1016/j.jbiomech.2022.111023.

Femoral version deformities alter joint reaction forces in dysplastic hips during gait

Molly C. Shepherd[a], **Brecca M.M. Gaffney**[b], **Ke Song**[c], **John C. Clohisy**[d], **Jeffrey J. Nepple**[d], **Michael D. Harris**[a,c,d,*]

[a]Program in Physical Therapy, Washington University School of Medicine, St. Louis, MO, USA

[b]Department of Mechanical Engineering, University of Colorado-Denver, Denver, CO, USA

[c]Department of Mechanical Engineering and Materials Science, Washington University in St. Louis, St. Louis, MO, USA

[d]Department of Orthopaedic Surgery, Washington University School of Medicine, St. Louis, MO, USA

Abstract

Developmental dysplasia of the hip (DDH) causes hip instability and early-onset osteoarthritis. The focus on pathomechanics in DDH has centered on the shallow acetabulum, however there is growing awareness of the role of femoral deformities in joint damage. The objective of this study was to determine the influence of femoral version (FV) on the muscle and joint reaction forces (JRFs) of dysplastic hips during gait. Magnetic resonance images, in-vivo gait data, and musculoskeletal models were used to calculate JRFs and simulate changes due to varying FV deformities. Rotation about the long axis of the femur was added in the musculoskeletal models to simulate FV values from −5°(relative retroversion) to + 35°(increased anteversion). In our simulations, FV deformities caused the largest changes to the anteroposterior and resultant JRFs. From a normal FV of 15°, a 15°increase in femoral anteversion caused JRFs to be less posterior in early stance (Δ = 0.43 ± 0.22 xbodyweight) and more anterior in late stance (Δ = 0.60 ± 14 xbodyweight). Relative retroversion caused anteroposterior changes that were similar to anteversion in early stance but opposite in late stance. Resultant JRFs experienced the largest changes during late stance where anteversion raised the peak by 0.48 ± 0.15 xbodyweight and relative retroversion lowered the peak by 0.32 ± 0.30 xbodyweight. Increasing anteversion increased hip flexor and abductor muscle forces, which caused the changes in JRFs. Identifying how FV deformities influence hip joint loading can elucidate their role in the mechanisms of hip degeneration in patients with DDH.

*Corresponding author at: 4444 Forest Park Avenue, Suite 1101, Campus Box 8502, St. Louis, MO 63108-2212, USA. harrismi@wustl.edu (M.D. Harris).

CRediT authorship contribution statement

Molly C. Shepherd: Conceptualization, Data curation, Formal analysis, Methodology, Writing – original draft, Writing – review & editing. **Brecca M.M. Gaffney**: Conceptualization, Data curation, Methodology, Writing – review & editing. **Ke Song**: Data curation, Methodology, Software, Writing – review & editing. **John C. Clohisy**: Data curation, Methodology, Supervision, Writing – review & editing. **Jeffrey J. Nepple**: Methodology, Resources, Writing – review & editing. **Michael D. Harris**:.

Declaration of Competing Interest

The authors declare that they have no known competing financial interests or personal relationships that could have appeared to influence the work reported in this paper.

Keywords

Femoral version; Joint reaction forces; Developmental dysplasia of the hip; Musculoskeletal modeling; Gait

1. Introduction

Developmental dysplasia of the hip (DDH) is characterized by skeletal deformities that cause abnormal articulation between the acetabulum and femoral head (Clohisy et al., 2009; van Bosse et al., 2015). Specifically, skeletal deformities in DDH increase loading at the anterolateral acetabular edge (Henak et al., 2014; Song et al., 2021), and cause unusually high muscle-induced joint reaction forces (JRFs) during gait (Harris et al., 2017; Song et al., 2020). As a result, patients with DDH often experience chondrolabral damage and are at a high risk for early development of osteoarthritis (Murphy et al., 1995).

The focus of clinical diagnosis and intervention for DDH remains on the abnormal acetabular structure. Patients with DDH have a shallow acetabulum which reduces coverage of the femoral head and is often considered to be the primary cause of instability and abnormal loading (van Bosse et al., 2015). However, femoral deformities occur in over 90% of hips with DDH and may include altered head-neck offset, coxa vara/valga, asphericity of the femoral head, and altered femoral version (Clohisy et al., 2009; Gaffney et al., 2019; Lerch et al., 2018; Wells et al., 2017). Despite increased recognition of femoral deformities, relatively little is known about how they influence loading in dysplastic hips and there is no consensus for their clinical management.

Femoral version (FV) deformities are among the most common in DDH. FV is measured as the angle between the femoral neck axis and the posterior condylar axis with FV values in healthy adults averaging approximately 15° (Fritz et al., 2018; Lerch et al., 2018; Mei-Dan et al., 2014; Murphy et al., 1987; Wells et al., 2017). FV angles above the normal range of 10° to 25° indicate increased anteversion while FV angles below that range are considered relative retroversion (Lerch et al., 2018; Wells et al., 2017). It is estimated that 64% of patients with DDH have FV deformities, with increased anteversion being more common than relative retroversion (Lerch et al., 2018). Musculoskeletal models have suggested that FV deformities can increase frontal plane muscle moments and hip contact forces in non-dysplastic hips (Heller et al., 2001; Kainz et al., 2020; Modenese et al., 2021) and may complicate joint reduction in infants with DDH (Huayamave et al., 2020). Despite insight gained from prior studies, the biomechanical implications of FV variability in dysplastic hips during common activities of daily living, such as gait, have not been reported.

The objective of this study was to determine the impact of FV on hip JRFs and muscle forces in patients with DDH during gait. To meet this objective, we used musculoskeletal modeling to simulate normal and deformed FV values ranging from increased anteversion to relative retroversion. Based on prior work we hypothesized that increased anteversion would increase loading in the hip joint (Heller et al., 2001; Kainz et al., 2020; Li et al., 2014; Modenese et al., 2021). We further hypothesized that increased anteversion would create larger changes than relative retroversion to hip muscle forces and JRFs.

2. Methods

2.1. Subjects and data collection

Fourteen female patients with symptomatic DDH were included in the current study (ages 26.5 ± 7.7 years; BMI 22.8 ± 2.5 kg/m^2). Hip JRFs during gait for these subjects were previously reported (Song et al., 2020). Patients were enrolled with Institutional Review Board approval and informed consent. All patients were diagnosed with DDH by a single orthopaedic surgeon based on acetabular lateral center edge angles (LCEA) less than 20° (LCEA = 10.2 ± 9.5°) (Delaunay et al., 1997) and unilateral hip/groin pain for at least 3 months. Exclusion criteria included previous hip surgery or infection, or secondary hip disorders such as Legg-Calves-Perthes disease, slipped capital femoral epiphysis, or femoroacetabular impingement.

MRI data from the psoas origin to the knee were collected as described previously, using a 3T scanner (VIDA; Siemens AG, Munich, Germany) and T1 weighted gradient-echo sequences (1×1×1 mm voxels) (Song et al., 2020). Kinematic data for each patient during gait were recorded at 100 Hz using 70 reflective markers and 10 infrared cameras (Vicon; Centennial, CO) (Song et al., 2020). Ground reaction forces were collected at 2000 Hz from force plates embedded in an instrumented treadmill (Bertec; Columbus, OH) at each patient's self-selected walking speed (Song et al., 2020).

2.2. Baseline musculoskeletal modeling

Baseline subject-specific musculoskeletal models were created for each patient as previously described (Song et al., 2020). Briefly, a 23 degree-of-freedom, 92 musculotendon actuator OpenSim musculoskeletal model (Lai et al., 2017) was modified for each patient by incorporating subject-specific pelvis and femur reconstructions from MRI. Thus, these baseline models represented each patient's native FV values, which ranged from − 4.8 to 33.5°. Subject-specific hip joint centers were updated in the model by applying a sphere fit to the MRI-reconstructed femoral heads (Harris et al., 2017). All other model segments were scaled using distances between skin-markers. Hip muscle attachment sites on the pelvis and femurs were updated based on MRI and bony geometry.

A representative gait cycle for each patient's symptomatic limb was used for analysis. Beginning with the baseline models, inverse kinematics was used to calculate subject-specific joint angles while minimizing spatial errors between experimental and model markers. A residual reduction algorithm was applied to improve dynamic consistency between the model's kinematics and the ground reaction forces and moments (Delp et al., 2007). Computed muscle control optimization was then used to calculate muscle forces (Thelen et al., 2003) and the OpenSim Joint Reaction Analysis tool was used to calculate hip JRFs in the pelvis reference frame to represent loading on the acetabulum. Consistent with published standards, we verified that residual forces and moments were minimized to recommended levels (Hicks et al., 2015). Muscle activation timing during gait was checked for qualitative agreement with surface EMG signals collected from the patients for eight bilateral lower extremity muscles (Supplementary Fig. 1). Across the range of FV values,

we also verified the absence of muscle wrapping anomalies such as muscles passing through bone, which can create unrealistic simulations.

2.3. FV deformity simulation

FV values were simulated in one degree increments between − 5° to + 35°. This range represented two standard deviations from the average FV measured from an in-house DDH database and fell within the range of FV values previously reported for patients with DDH (Murphy et al., 1987) (Supplementary Fig. 2). First, femurs of the symptomatic limb were transected at the most distal point of the lesser trochanter in accordance with the subtrochanteric origin of many FV deformities (Archibald et al., 2019; Fritz et al., 2018; Waisbrod et al., 2017) and surgical cut locations to correct for femoral deformities (Buly et al., 2018; Georgiadis et al., 2015) (Fig. 1). Next, a rotational degree-of-freedom was added at the transection point between the proximal and distal femur segments to allow rotation about the long axis of the femur. The degree-of-freedom was unlocked and the lower limb distal to the lesser trochanter was rotated, including the distal part of the femur, the shank and foot, and all muscle attachments. After rotating the femur to a new FV value, the rotational degree-of-freedom was locked and muscle tendon slack lengths and optimal fiber lengths were scaled relative to changes in muscle length due to the rotation (Song et al., 2020; Wesseling et al., 2016). Inverse kinematics were re-run, which allowed the entire lower limb to rotate and return the foot position to its original alignment with the experimental ground reaction forces. The original location of the hip joint center relative to the ground reaction forces was also preserved, which kept the net hip joint moments the same regardless of FV changes. With each FV iteration, hip joint angles were defined between the coordinate system of the proximal femur segment and the pelvis. The residual reduction algorithm and computed muscle control were then run to calculate new muscle forces and JRFs across the gait cycle (Fig. 1). This process was repeated for each patient and each FV value in the −5° to + 35° range, resulting in 41 models per patient. All FV deformity iterations for each patient were run in parallel using the high throughput Open Science Grid (Pordes et al., 2007; Sfiligoi et al., 2009). Pearson correlation coefficients (moderate: $0.4 \leq r < 0.6$, strong: $r \geq 0.6$) (Myers et al., 2015) were used to calculate the sensitivity between FV values and the corresponding JRFs or muscle forces for each patient at the times of peak JRF in early stance (JRF1) and late stance (JRF2). Lines were fit to the FV versus force points and their slopes were used to predict force changes given a 15° increase or decrease in FV away from the normal FV of 15° (Gaffney et al., 2020).

3. Results

3.1. Joint reaction forces

All hip JRFs were strongly sensitive to FV variability in our models (Table 1, Supplementary Fig. 3). With progressively increasing femoral anteversion, there was a corresponding increase in resultant, anterior, and superior JRFs at JRF1 and JRF2, but a decrease in the medial JRF component (Fig. 2). Conversely, relative retroversion decreased resultant, anterior, and superior JRFs at JRF2, but increased the resultant, superior, and medial JRFs at JRF1 (Fig. 2).

Best-fit lines predicted that from the normal FV value of 15°, a 15° increase in anteversion caused a 0.19 ± 0.24 × bodyweight (xBW) increase (3.90 ± 4.73% change) in the resultant JRF in early stance (JRF1), while a 15° change toward relative retroversion caused an increase of 0.29 ± 0.44 xBW (5.52 ± 8.57% change) (Fig. 3). At the time of JRF2, 15° of increased anteversion or relative retroversion caused changes to the resultant JRF of +0.48 ± 0.15 xBW (8.87 ± 2.77% change) and −0.32 ± 0.30 xBW (5.50 ± 6.04% change), respectively (Fig. 3).

Among the JRF components, the anteroposterior (A/P) component experienced the largest changes with 15° of increased anteversion (ΔJRF1 = +0.43 ± 0.22 xBW, 191.09 ± 200.34% change; ΔJRF2 = +0.60 ± 0.14 xBW, 29.10 ± 14.34% change) or relative retroversion (ΔJRF1 = −0.65 ± 0.28 xBW, 248.10 ± 182.38% change; ΔJRF2 = −0.67 ± 0.45 xBW, 32.77 ± 30.49% change) (Fig. 3). The superoinferior (S/I) component increased with increased anteversion at both JRF1 and JRF2 (ΔJRF1 = +0.25 ± 0.18 xBW, 5.04 ± 3.79% change; ΔJRF2 = +0.26 ± 0.17 xBW, 5.51 ± 3.71% change). S/I forces also increased at JRF1with relative retroversion (ΔJRF1 = +0.12 ± 0.36 xBW, 2.74 ± 7.69% change), but then dropped at JRF2 (ΔJRF2 = −0.16 ± 0.33 xBW, 3.14 ± 7.70% change). For the mediolateral (M/L) JRF component, changes caused by 15° of increased anteversion or relative retroversion were nearly symmetric at JRF1 and JRF2 and minor compared to the other JRF components (Fig. 3).

3.2. Muscle forces

Increased femoral anteversion increased most primary hip abductor and flexor muscle forces (grouped according to Neumann 2010) (Fig. 4, Supplementary Table 1) (Neumann, 2010). Relative retroversion decreased most abductor and flexor forces, and increased extensor forces. An exception was the anterior section of the gluteus medius at JRF2, whose forces decreased with anteversion and increased with relative retroversion. The largest muscle force changes occurred at JRF2 where 15° of increased anteversion raised the iliacus, rectus femoris, and tensor fascia latae by 0.14 ± 0.06 xBW (15.45 ± 13.12% change), 0.13 ± 0.09 xBW (23.67 ± 27.79% change), and 0.13 ± 0.07 xBW (35.81 ± 14.73% change), respectively, and relative retroversion raised anterior gluteus medius forces by 0.17 ± 0.14 (16.92 ± 17.06% change) (Fig. 4, Supplementary Table 1). Hip extensor forces mostly decreased with anteversion at JRF1 and had a mixed response at JRF2; extensor changes at JRF1 and JRF2 were also mixed with relative retroversion (Fig. 4). Changes to muscle forces of the primary internal and external rotators were less than 0.075 xBW, with the exception of the anterior gluteus medius at JRF2, and the gemellus, which increased at JRF1 and JRF2 with relative retroversion (Supplementary Fig. 4).

3.3. Kinematics and muscle moment arms

Changing FV values and re-running inverse kinematics to maintain the original foot position relative to the ground reaction force had the largest effect on internal and external hip rotation. Hips for all patients became externally rotated with increased anteversion and internally rotated with relative retroversion (Supplementary Fig. 5). Hip flexion–extension and abduction–adduction remained unchanged by the changing FV values (Supplementary Fig. 5).

Changes to FV values and hip internal-external rotation caused small changes to the abduction and extension moment arms of the primary abductors (Supplementary Figs. 6a & b). Specifically, abduction moment arms of the anterior, middle, and posterior sections of the gluteus medius and gluteus minimus decreased with increased anteversion and external hip rotation. Conversely, extension moment arms of the abductors increased with increased anteversion and external hip rotation.

4. Discussion

The objective of this study was to determine the impact of FV on hip JRFs and muscle forces in patients with DDH during gait. We found that increasing femoral anteversion increased the resultant, anterior, and superior hip JRFs while decreasing medial JRFs in both early and late stance. Additionally, our results indicated that increased anteversion generally increased muscle forces, which had the largest effect on the hip flexors and most hip abductors in late stance. In general, relative retroversion had opposite effects on hip JRFs and muscle forces as anteversion, with the exception of an increase in the superior and resultant JRFs in early stance.

Our results suggest that increased femoral anteversion elevates resultant, anterior, and superior JRFs, which may contribute to damaging articular loads in dysplastic hips. Increased anteversion caused the largest change to anterior JRFs, primarily in late stance when joint loading is directed anteriorly. At that time point, a 15° increase in anteversion from the normal FV of 15° raised the anterior JRF by 29%. Acetabular labral damage in patients with DDH most commonly occurs in the anterior/anterosuperior region of the acetabulum (Leunig et al., 2004; Tamura et al., 2013). Given that articular stresses are disproportionately carried by the anterosuperior labrum in dysplastic hips (Henak et al., 2014), the increased anterior and superior JRFs from excessive anteversion will increase the risk for chondrolabral damage. Our results suggest a steady increase in that risk with increasing anteversion. Because no clinical studies have investigated correlations between the degree of FV deformity in DDH and chondrolabral damage, future studies will need to establish what level of risk can be a prognosticator of detectable damage.

We also found that increased anteversion reduced medial JRFs, especially in early stance, which was surprising given previous work that showed patients with DDH experienced higher medial JRFs than healthy controls during that phase of gait (Harris et al., 2017; Song et al., 2020). However, previous studies reporting JRFs in dysplastic hips did not explicitly report femoral deformities or their influence (Harris et al., 2017; Skalshøi et al., 2015; Song et al., 2020). Consistent with our results, other studies have found that with increased anteversion, the femoral head is often externally rotated in the acetabulum, which is associated with shorter abductor moment arms (Arnold et al., 1997; Scorcelletti et al., 2020). The external rotation causes abductor muscle lines of action, especially of the gluteus minimus and medius to become more posterior than lateral, thereby reducing their contribution to medial JRFs and potentially increasing contributions to anterior JRFs. While our models suggest that increased anteversion may reduce medial JRFs during gait, the changes are small. Indeed, despite the reduced medial JRFs, simulated excessive anteversion in the current study increased the anterior and superior JRFs enough to ultimately raise

the resultant JRF. These results help illustrate the role of FV in biomechanical trade-offs between medial JRFs that stabilize dysplastic hips but may contribute to medial femoral damage, and anterosuperior JRFs that can contribute to acetabular chondrolabral damage.

Our findings corroborate previous musculoskeletal simulations of FV changes in non-dysplastic hips. Specifically, our results and those of previous studies found that hip JRFs are highly sensitive to FV changes and resultant JRFs increase with increasing anteversion (Heller et al., 2001; Kainz et al., 2020; Modenese et al., 2021). Although individual muscle forces were not reported in previous simulations of FV, they can provide further explanation of the JRF changes. As mentioned, external rotation of the proximal femur with increased anteversion led to a decrease in abductor muscle moment arms (Arnold et al., 1997; Scorcelletti et al., 2020), meaning that greater forces must be generated to meet the torque demands required for joint stabilization. This force compensation was seen in the increased abductor forces; however, it does not explain the decrease in extensor forces in early stance. The decrease in extensor forces with increased anteversion may be due to the abductors becoming more posterior with the external rotation of the proximal femur, and therefore taking on some of the role of the extensor muscles. Increased flexor forces during late stance coincided with, and were likely in response to, changes from muscles directly affected by FV alterations (e.g. anterior gluteus medius, tensor fascia latae). For example, abduction and flexion moment arms of the tensor fascia latae shortened with increased anteversion, thereby reducing the muscle's effectiveness in both roles. However, the net joint moment to be satisfied in late stance remained the same. Thus, despite tensor fascia latae forces increasing with anteverison, increased rectus femoris and iliacus forces may have been needed to fully stabilize and move the hip. These compensations, found through simulation, can further refine our understanding of how DDH alters the primary and secondary functions of hip muscles that underlie JRFs (Song et al., 2020).

Understanding the influence of FV deformities on hip JRFs can inform clinical diagnosis and decision making. Currently, there is no standardization or consensus for surgeons to decide if or how to address FV deformity in the context of DDH. This is due largely to the lack of quantitative information about the biomechanical influence of FV. Knowing the increase in anterior or superior JRFs with increasing FV anteversion can help clinicians more fully understand the biomechanical profile of their patients. Future work can simulate surgical correction of FV deformities and estimate the magnitude of resulting biomechanical changes.

It is unclear how the changes to JRFs and muscle forces with relative retroversion may influence clinical presentation of patients with DDH. Relative retroversion is less common than increased anteversion in this population (Lerch et al., 2018; Wells et al., 2017), and similar to anteversion there is a paucity of studies investigating retroversion and joint damage. In our findings, relative retroversion frequently had the opposite effect of increased anteversion. For example, medial JRFs were slightly larger with relative retroversion and were accompanied by higher forces from the anterior section of the gluteus medius, which contrasted with the reduced medial JRFs of anteversion. Also, except at the peak loads in early stance, JRFs became more posterior and less superior, which agrees with cadaveric studies that found relative retroversion shifts cartilage stresses posteroinferiorly (Satpathy

et al., 2015). Relative retroversion may increase risk for femoracetabular impingement (Matsuda et al., 2014; Satpathy et al., 2015). Thus, while the impact of relative retroversion on joint damage in untreated dysplastic hips is still unknown, its mechanical effects should be considered when planning acetabular reorientation surgery to avoid secondary impingement (Pascual-Garrido et al., 2017).

There were limitations that should be taken into consideration when interpreting the results of this study. First, by allowing the leg to rotate after simulating each FV value, we did not alter foot progression angles when simulating FV deformities. This approach avoided mismatches between the foot and the ground reaction forces. It has been shown that while patients with negative foot progression angles (indicating in-toeing) often have increased femoral anteversion, most patients with abnormal femoral anteversion have normal foot progression angles (Lerch et al., 2019). Thus, we maintained each patient's original foot progression angles and allowed rotational changes primarily at the hip. Changes in FV may be counteracted by a combination of tibial torsion and hip rotation, although there is a lack of consensus on the contributions of each. Second, we simulated FV deformity immediately distal to the lesser trochanter which was supported by previous reports of the origin of FV deformities (Archibald et al., 2019; Fritz et al., 2018; Waisbrod et al., 2017). However, there have been conflicting reports on FV deformity origination and where surgical correction should be performed along the femur (Archibald et al., 2019; Buly et al., 2018; Fritz et al., 2018; Fuller et al., 2018; Hartigan et al., 2017; Heller et al., 2001; Mei-Dan et al., 2014). Third, we scaled tendon slack length and optimal fiber length relative to the change in muscle length with each FV change. This method assumes that the muscles have the same operating range relative to the muscles' length at an anatomical neutral standing position. While there are different methods to update these parameters, a recent study that modeled FV and found similar trends as our study, also found no significant differences in hip JRF estimates between models that did and did not update musculotendon parameters (Modenese et al., 2021). Therefore, we found our method to be appropriate for our study objective. Fourth, we did not have in-vivo data to fully validate our baseline models or changes to JRFs and muscle forces with FV alterations. Although we followed established validation practices, true validation is a challenge with musculoskeletal modeling, and results should be interpreted with caution. However, because our objective was to report JRF and muscle force changes with FV, the trends found can be valuable for assessing the impact of FV deformities.

In conclusion, our study found that the strongest influence on hip JRFs came from increased femoral anteversion among patients with DDH. These findings can help explain mechanisms of damage reported in dysplastic hips. Understanding the relationship between the acetabulum and femur geometries in DDH, as well as their corresponding joint biomechanics, can help identify patients' risks for damage and inform surgical or movement-based correction for improved joint preservation outcomes and osteoarthritis prevention.

Supplementary Material

Refer to Web version on PubMed Central for supplementary material.

Acknowledgements

This project was supported by the National Institutes of Health K01AR072072, P30AR074992, F32AR075349, T32HD007434, and the American Society of Biomechanics Junior Faculty Research Award. The research content herein is solely the responsibility of the authors and does not necessarily represent the official views of the National Institutes of Health. This research was done using resources provided by the Open Science Grid (Pordes et al., 2007; Sfiligoi et al., 2009), which is supported by the National Science Foundation award #2030508.

References

Archibald HD, Petro KF, Liu RW, 2019. An anatomic study on whether femoral version originates in the neck or the shaft. J. Pediatric Orthopaedics 39 (1), e50–e53. 10.1097/BPO.0000000000001070.

Arnold AS, Komattu A. v, & Delp SL (1997). Internal rotation gait : a compensatory mechanism to restore abduction capacity deformity ? Dev Med Child Neurol, 39(1), 40–44. [PubMed: 9003728]

Buly RL, Sosa BR, Poultsides LA, Caldwell E, Rozbruch SR, 2018. Femoral Derotation Osteotomy in Adults for Version Abnormalities. J. Am. Academy Orthopaedic Surgeons 26 (19), e416–e425. 10.5435/JAAOS-D-17-00623.

Clohisy JC, Nunley RM, Carlisle JC, Schoenecker PL, 2009. Incidence and characteristics of femoral deformities in the dysplastic hip. Clin. Orthop. Relat. Res 467 (1), 128–134. 10.1007/s11999-008-0481-3. [PubMed: 19034600]

Delaunay S, Dussault RG, Kaplan PA, Alford BA, 1997. Radiographic measurements of dysplastic adult hips. Skeletal Radiol 26 (2), 75–81. 10.1007/s002560050197. [PubMed: 9060097]

Delp SL, Anderson FC, Arnold AS, Loan P, Habib A, John CT, Guendelman E, Thelen DG, 2007. OpenSim: Open-source software to create and analyze dynamic simulations of movement. IEEE Trans. Biomed. Eng 54 (11), 1940–1950. 10.1109/TBME.2007.901024. [PubMed: 18018689]

Fritz B, Bensler S, Leunig M, Zingg PO, Pfirrmann CWA, Sutter R, 2018. MRI Assessment of Supra- and Infratrochanteric Femoral Torsion: Association With Femoroacetabular Impingement and Hip Dysplasia. Am. J. Roentgenol 211 (1), 155–161. 10.2214/AJR.17.18882. [PubMed: 29733696]

Fuller CB, Farnsworth CL, Bomar JD, Jeffords ME, Murphy JS, Edmonds EW, Pennock AT, Wenger DR, & Upasani V. v. (2018). Femoral version: Comparison among advanced imaging methods. Journal of Orthopaedic Research, 36 (5), 1536–1542. 10.1002/jor.23785. [PubMed: 29077224]

Gaffney BMM, Clohisy JC, Van Dillen LR, Harris MD, 2020. The association between periacetabular osteotomy reorientation and hip joint reaction forces in two subgroups of acetabular dysplasia. J. Biomech 98, 109464. 10.1016/j.jbiomech.2019.109464. [PubMed: 31708245]

Gaffney BMM, Hillen TJ, Nepple JJ, Clohisy JC, Harris MD, 2019. Statistical shape modeling of femur shape variability in female patients with hip dysplasia. J. Orthop. Res 37 (3), 665–673. 10.1002/jor.24214. [PubMed: 30656719]

Georgiadis AG, Siegal DS, Scher CE, Zaltz I, 2015. Can Femoral Rotation Be Localized and Quantified Using Standard CT Measures? Clin. Orthop. Relat. Res 473 (4), 1309–1314. 10.1007/s11999-014-4000-4. [PubMed: 25337975]

Harris MD, MacWilliams BA, Bo Foreman K, Peters CL, Weiss JA, Anderson AE, 2017. Higher medially-directed joint reaction forces are a characteristic of dysplastic hips: A comparative study using subject-specific musculoskeletal models. J. Biomech 54, 80–87. 10.1016/j.jbiomech.2017.01.040. [PubMed: 28233552]

Hartigan DE, Perets I, Walsh JP, Domb BG, 2017. Femoral Derotation Osteotomy Technique for Excessive Femoral Anteversion. Arthroscopy Techniques 6 (4), e1405–e1410. 10.1016/j.eats.2017.05.027. [PubMed: 29354448]

Heller MO, Bergmann G, Deuretzbacher G, Claes L, Haas NP, Duda GN, 2001. Influence of femoral anteversion on proximal femoral loading: Measurement and simulation in four patients. Clin. Biomech 16 (8), 644–649. 10.1016/S0268-0033(01)00053-5.

Henak CR, Abraham CL, Anderson AE, Maas SA, Ellis BJ, Peters CL, Weiss JA, 2014. Patient-specific analysis of cartilage and labrum mechanics in human hips with acetabular dysplasia. Osteoarthritis Cartilage 22 (2), 210–217. 10.1016/j.joca.2013.11.003. [PubMed: 24269633]

Hicks JL, Uchida TK, Seth A, Rajagopal A, Delp SL, 2015. Is My Model Good Enough? Best Practices for Verification and Validation of Musculoskeletal Models and Simulations of Movement. J. Biomech. Eng 137 (2) 10.1115/1.4029304.

Huayamave V, Lozinski B, Rose C, Ali H, Kassab A, Divo E, Moslehy F, Price C, 2020. Biomechanical evaluation of femoral anteversion in developmental dysplasia of the hip and potential implications for closed reduction. Clin. Biomech 72, 179–185.

Kainz H, Killen BA, Wesseling M, Perez-Boerema F, Pitto L, Garcia Aznar JM, Shefelbine S, Jonkers I, Zhang X, 2020. A multi-scale modelling framework combining musculoskeletal rigid-body simulations with adaptive finite element analyses, to evaluate the impact of femoral geometry on hip joint contact forces and femoral bone growth. PLoS ONE 15 (7), e0235966. 10.1371/journal.pone.0235966. [PubMed: 32702015]

Lai AKM, Arnold AS, Wakeling JM, 2017. Why are Antagonist Muscles Co-activated in My Simulation? A Musculoskeletal Model for Analysing Human Locomotor Tasks. Ann. Biomed. Eng 45 (12), 2762–2774. 10.1007/s10439-017-1920-7. [PubMed: 28900782]

Lerch TD, Eichelberger P, Baur H, Schmaranzer F, Liechti EF, Schwab JM, Siebenrock KA, Tannast M, 2019. Prevalence and diagnostic accuracy of in-toeing and out-toeing of the foot for patients with abnormal femoral torsion and femoroacetabular impingement: Implications for hip arthroscopy and femoral derotation osteotomy. Bone Joint J 101-B (10), 1218–1229. 10.1302/0301-620X.101B10.BJJ-2019-0248.R1. [PubMed: 31564157]

Lerch TD, Todorski IAS, Steppacher SD, Schmaranzer F, Werlen SF, Siebenrock KA, Tannast M, 2018. Prevalence of Femoral and Acetabular Version Abnormalities in Patients With Symptomatic Hip Disease: A Controlled Study of 538 Hips. Am. J. Sports Med 46 (1), 122–134. 10.1177/0363546517726983. [PubMed: 28937786]

Leunig M, Podeszwa D, Beck M, Werlen S, Ganz R, 2004. Magnetic Resonance Arthrography of Labral Disorders in Hips with Dysplasia and Impingement. Clin. Orthop. Relat. Res 418, 74–80. 10.1097/00003086-200401000-00013.

Li H, Wang Y, Oni JK, Qu X, Li T, Zeng Y, Liu F, Zhu Z, 2014. The role of femoral neck anteversion in the development of osteoarthritis in dysplastic hips. Bone Joint J 96B (12), 1586–1593. 10.1302/0301-620X.96B12.33983.

Matsuda DK, Gupta N, Martin HD, 2014. Closed intramedullary derotational osteotomy and hip arthroscopy for cam femoroacetabular impingement from femoral retroversion. Arthroscopy Techniques 3 (1), e83–e88. 10.1016/j.eats.2013.08.013. [PubMed: 24749047]

Mei-Dan O, McConkey MO, Bravman JT, Young DA, Pascual-Garrido C, 2014. Percutaneous femoral derotational osteotomy for excessive femoral torsion. Orthopedics 37 (4), 243–249. 10.3928/01477447-20140401-06. [PubMed: 24762832]

Modenese L, Barzan M, Carty CP, 2021. Dependency of Lower Limb Joint Reaction Forces on Femoral Anteversion. Gait & Posture 88 (February), 318–321. 10.1016/j.gaitpost.2021.06.014. [PubMed: 34246172]

Murphy SB, Ganz R, Muller ME, 1995. The prognosis in untreated dysplasia of the hip. A study of radiographic factors that predict the outcome. J. Bone Joint Surg 77 (7), 985–989. [PubMed: 7608241]

Murphy SB, Simon SR, Kijewski PK, Wilkinson RH, Griscom NT, 1987. Femoral Anteversion. J. Bone Joint Surg 69 (8), 1169–1176. [PubMed: 3667647]

Myers CA, Laz PJ, Shelburne KB, Davidson BS, 2015. A Probabilistic Approach to Quantify the Impact of Uncertainty Propagation in Musculoskeletal Simulations. Ann. Biomed. Eng 43 (5), 1098–1111. 10.1007/s10439-014-1181-7. [PubMed: 25404535]

Neumann DA, 2010. Kinesiology of the hip: A focus on muscular actions. J. Orthop. Sports Phys. Ther 40 (2), 82–94. 10.2519/jospt.2010.3025. [PubMed: 20118525]

Pascual-Garrido C, Harris MD, Clohisy JC, 2017. Innovations in Joint Preservation Procedures for the Dysplastic Hip “The Periacetabular Osteotomy”. J. Arthroplasty 32 (9), S32–S37. 10.1016/j.arth.2017.02.015. [PubMed: 28318866]

Pordes R, Petravick D, Kramer B, Olson D, Livny M, Roy A, Avery P, Blackburn K, Wenaus T, Würthwein F, Foster I, Gardner R, Wilde M, Blatecky A, McGee J, Quick R, 2007. The open science grid. J. Phys. Conf. Ser 78, 012057. 10.1088/1742-6596/78/1/012057.

Satpathy J, Kannan A, Owen JR, Wayne JS, Hull JR, Jiranek WA, 2015. Hip contact stress and femoral neck retroversion: a biomechanical study to evaluate implication of femoroacetabular impingement. J. Hip Preservation Surgery 2 (3), 287–294. 10.1093/jhps/hnv040.

Scorcelletti M, Reeves ND, Rittweger J, Ireland A, 2020. Femoral anteversion: significance and measurement. J. Anat 237 (5), 811–826. 10.1111/joa.13249. [PubMed: 32579722]

Sfiligoi I, Bradley DC, Holzman B, Mhashilkar P, Padhi S, & Würthwein F (2009). The pilot way to Grid resources using glideinWMS. 2009 WRI World Congress on Computer Science and Information Engineering, CSIE 2009, 2, 428–432. 10.1109/CSIE.2009.950.

Skalshøi O, Iversen CH, Nielsen DB, Jacobsen J, Mechlenburg I, Søballe K, Sørensen H, 2015. Walking patterns and hip contact forces in patients with hip dysplasia. Gait and Posture 42 (4), 529–533. 10.1016/j.gaitpost.2015.08.008. [PubMed: 26365370]

Song K, Gaffney BMM, Shelburne KB, Pascual-Garrido C, Clohisy JC, Harris MD, 2020. Dysplastic hip anatomy alters muscle moment arm lengths, lines of action, and contributions to joint reaction forces during gait. J. Biomech 110, 109968. 10.1016/j.jbiomech.2020.109968. [PubMed: 32827786]

Song K, Pascual-Garrido C, Clohisy JC, Harris MD, 2021. Acetabular Edge Loading During Gait Is Elevated by the Anatomical Deformities of Hip Dysplasia. Frontiers Sports Active Living 3 (July), 1–9. 10.3389/fspor.2021.687419.

Tamura S, Nishii T, Takao M, Sakai T, Yoshikawa H, Sugano N, 2013. Differences in the locations and modes of labral tearing between dysplastic hips and those with femoroacetabular impingement. Bone Joint J 95-B (10), 1320–1325. 10.1302/0301-620X.95B10.31647. [PubMed: 24078526]

Thelen DG, Anderson FC, Delp SL, 2003. Generating dynamic simulations of movement using computed muscle control. J. Biomech 36 (3), 321–328. 10.1016/S0021-9290(02)00432-3. [PubMed: 12594980]

van Bosse H, Wedge JH, Babyn P, 2015. How Are Dysplastic Hips Different? A Three-dimensional CT Study. Clin. Orthop. Relat. Res 473 (5), 1712–1723. 10.1007/s11999-014-4103-y. [PubMed: 25524428]

Waisbrod G, Schiebel F, Beck M, 2017. Abnormal femoral antetorsion—a subtrochanteric deformity. J. Hip Preservation Surgery 4 (2), 153–158. 10.1093/jhps/hnx013.

Wells J, Nepple JJ, Crook K, Ross JR, Bedi A, Schoenecker P, Clohisy JC, 2017. Femoral Morphology in the Dysplastic Hip: Three-dimensional Characterizations With CT. Clin. Orthop. Relat. Res 475 (4), 1045–1054. 10.1007/s11999-016-5119-2. [PubMed: 27752989]

Wesseling M, de Groote F, Bosmans L, Bartels W, Meyer C, Desloovere K, Jonkers I, 2016. Subject-specific geometrical detail rather than cost function formulation affects hip loading calculation. Comput. Methods Biomech. Biomed. Eng 19 (14), 1475–1488. 10.1080/10255842.2016.1154547.

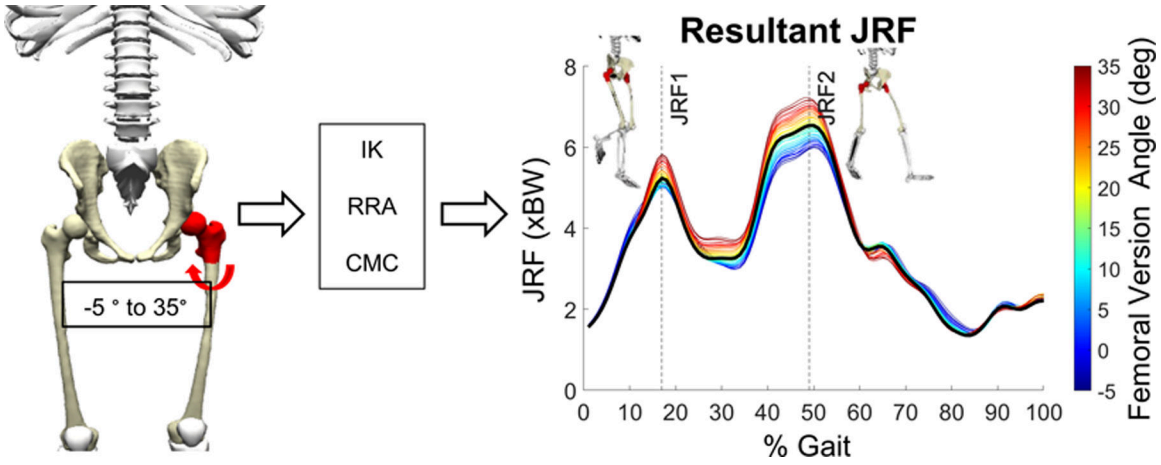

Fig. 1.

FV deformity simulation and modeling pipeline. A rotational degree-of-freedom was created in the symptomatic femur of each subject's model. FV deformities were then simulated by rotating the femur to a FV value between −5° and + 35°. For every simulated FV deformity, hip muscle and JRFs were recalculated. The process was repeated 41 times within the FV range to quantify the influence of the deformities on muscle and hip JRFs at the time points of peak JRF in early (JRF1) and late (JRF2) stance. IK = inverse kinematics; RRA = residual reduction analysis; CMC = computed muscle control.

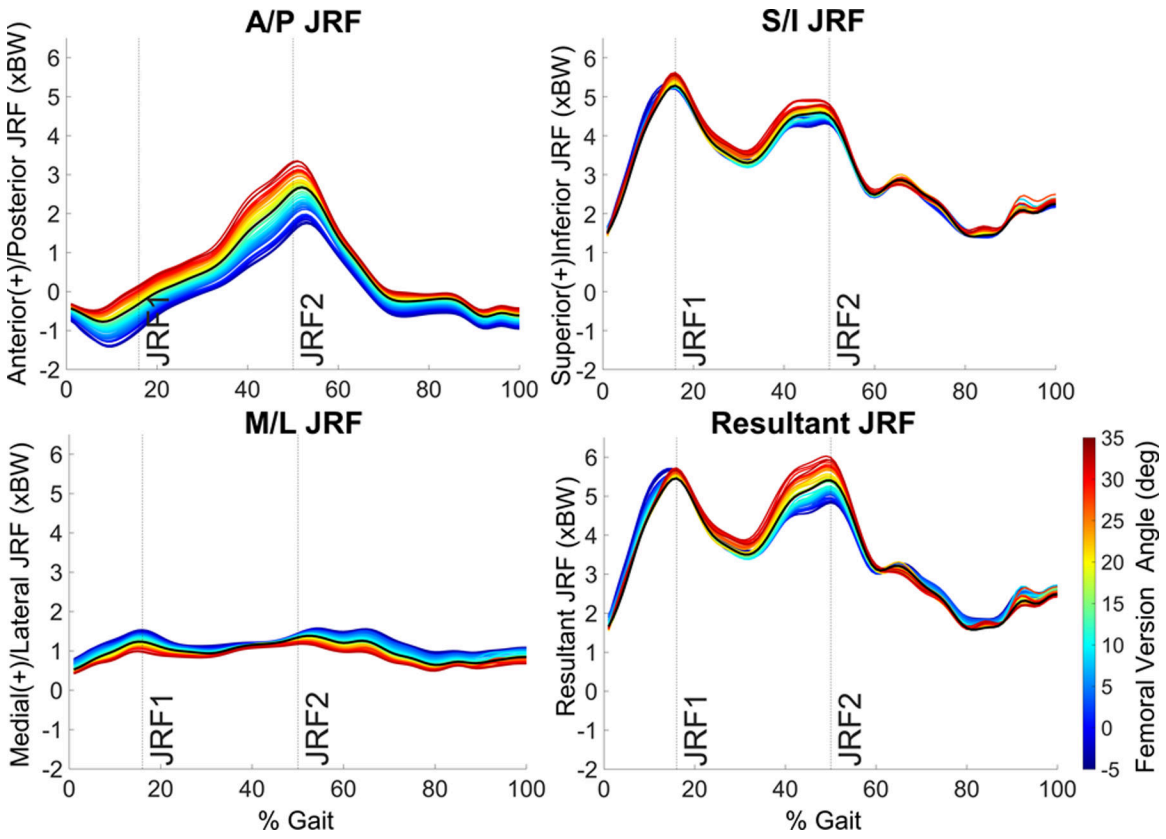

Fig. 2.

JRFs across the gait cycle averaged for all 14 patients. Each colored line represents a different femoral version angle from −5° to + 35°.

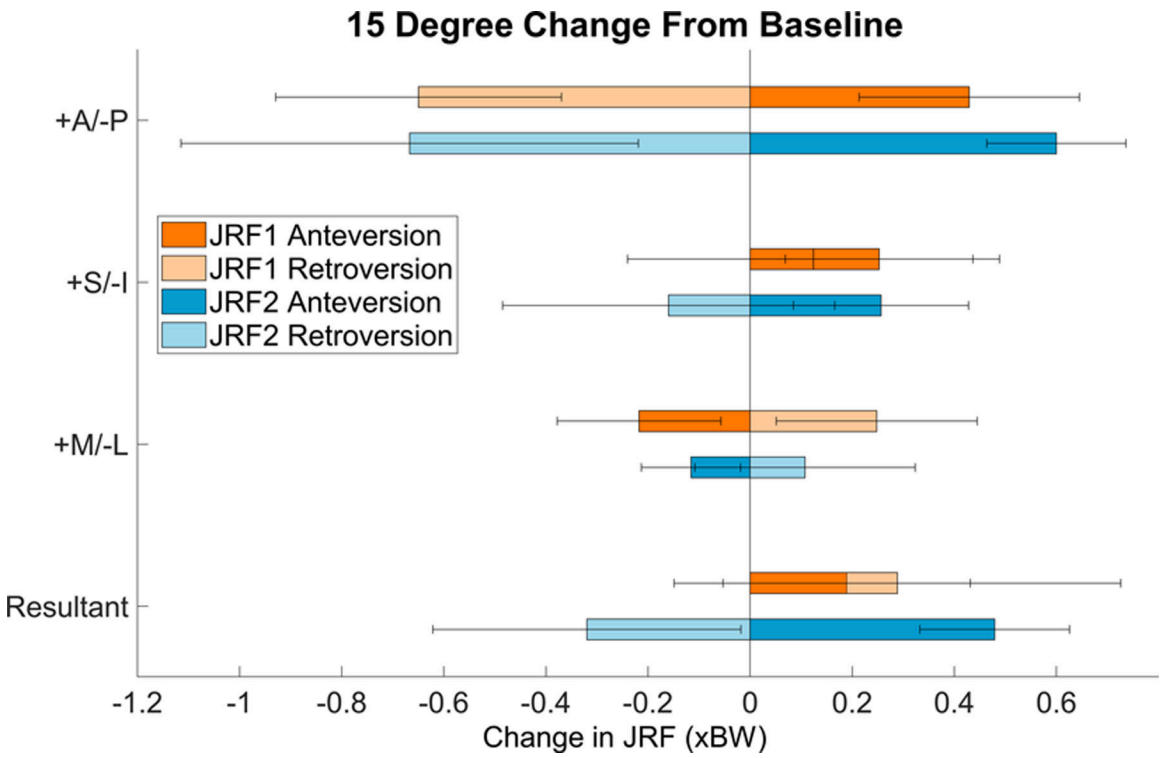

Fig. 3.

Average change in JRFs with 15° change in FV for the 14 patients. Orange indicates JRF1; blue indicates JRF2. Error bars = standard deviation.

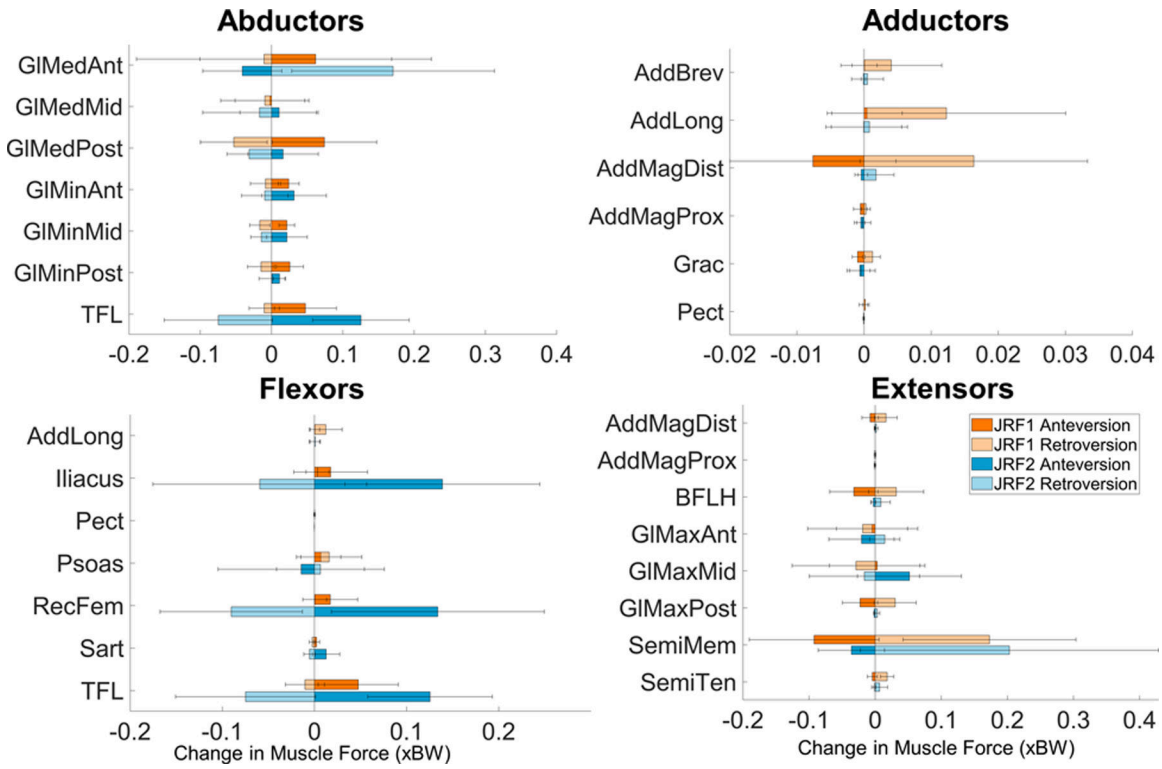

Fig. 4.

Average and standard deviation change in muscle forces around the hip with 15° change in FV deformity across the entire gait cycle for 14 patients. Increased anteversion primarily increased abductors and flexors and decreased extensors. Orange indicates JRF1; blue indicates JRF2. GlMed = gluteus medius; GlMin = gluteus minimus; TFL = tensor fascia latae; AddBrev = adductor brevis; AddLong = adductor longus; AddMag = adductor magnus; Grac = gracilis; Pect = pectineus; RecFem = rectus femoris; Sart = Sartorius; BFLH = biceps femoris long head; GlMax = gluteus maximus; SemiMem = semimembranosus; SemiTen = semitendinosus.

Table 1

Average ± standard deviation sensitivity factors (Pearson r) and slopes of predictive lines (xBW/°) at JRF1 and JRF2. Sensitivity factors and best-fit lines were determined for each JRF component and the resultant JRF.

		JRF1		JRF2	
		r	**slope**	**r**	**slope**
Ante	A/P	0.99±0.01	0.03±0.01	0.93±0.10	0.04±0.01
	S/I	0.92±0.06	0.02±0.01	0.74±0.31	0.02±0.01
	M/L	0.94±0.11	−0.01±0.01	0.77±0.31	−0.01±0.01
	Result.	0.78±0.28	0.01±0.01	0.90±0.25	0.03±0.01
Retro	A/P	0.97±0.07	0.04±0.02	0.87±0.25	0.04±0.03
	S/I	0.73±0.33	−0.01±0.02	0.74±0.25	0.01±0.02
	M/L	0.94±0.11	−0.02±0.01	0.71±0.27	−0.01±0.01
	Result.	0.78±0.30	−0.02±0.03	0.84±0.23	0.02±0.02